

AD-A076 152

PURDUE UNIV LAFAYETTE IND DEPT OF CHEMISTRY
SUPERCOOLED AND SUPERHEATED WATER.(U)
OCT 79 C A ANGELL

F/G 20/13

UNCLASSIFIED

N00014-78-C-0035
NL

1 OF 1

AD
A076152



END

DATE

FILMED

11-79

DDC

AD A076152

LEVEL

SUPERCOOLED AND SUPERHEATED WATER

C. A. Angell
Purdue University
Department of Chemistry
West Lafayette, Indiana 47907

DDC
RECEIVED
NOV 5 1979
E

October 1979

Technical Report, October 1979

Distribution Statement

Prepared for

Office of Naval Research
800 N. Quincy Street
Arlington, VA 22217

Division of Sponsored Programs
Purdue Research Foundation
Purdue University
West Lafayette, Indiana 47907

This document has been approved
for public release and sale; its
distribution is unlimited.

79 10 17 065

291 725

YB

DDC FILE COPY

| REPORT DOCUMENTATION PAGE | | READ INSTRUCTIONS BEFORE COMPLETING FORM |
|--|-----------------------|---|
| 1. REPORT NUMBER N00014-78-C-0035 | 2. GOVT ACCESSION NO. | 3. RECIPIENT'S CATALOG NUMBER |
| 4. TITLE (and Subtitle) Supercooled and Superheated Water | | 5. TYPE OF REPORT & PERIOD COVERED Technical Report, Oct. 1979 |
| | | 6. PERFORMING ORG. REPORT NUMBER |
| 7. AUTHOR(s) C. A. Angell | | 8. CONTRACT OR GRANT NUMBER(s) N78C0035 |
| 9. PERFORMING ORGANIZATION NAME AND ADDRESS Purdue University Department of Chemistry West Lafayette, IN 47907 | | 10. PROGRAM ELEMENT, PROJECT, TASK AREA & WORK UNIT NUMBERS |
| 11. CONTROLLING OFFICE NAME AND ADDRESS Office of Naval Research 800 N. Quincy Street Arlington, VA 22217 | | 12. REPORT DATE October 1979 |
| | | 13. NUMBER OF PAGES |
| 14. MONITORING AGENCY NAME & ADDRESS (if different from Controlling Office) Division of Sponsored Programs Purdue Research Foundation Purdue University West Lafayette, IN 47907 | | 15. SECURITY CLASS. (of this report) Unclassified |
| | | 15a. DECLASSIFICATION/DOWNGRADING SCHEDULE |
| 16. DISTRIBUTION STATEMENT (of this Report) | | |
| 17. DISTRIBUTION STATEMENT (of the abstract entered in Block 20, if different from Report) | | |
| 18. SUPPLEMENTARY NOTES This manuscript was prepared as the written version of an invited lecture at the 50th Anniversary of the 1st International Conference on the Properties of Steam, held in Munich, Germany, September 10-14, 1979. | | |
| 19. KEY WORDS (Continue on reverse side if necessary and identify by block number) Water; metastable; supercooled; superheated; heat capacities; anomalies | | |
| 20. ABSTRACT (Continue on reverse side if necessary and identify by block number) Various thermodynamic, transport and structural features of water in its metastable states, both supercooled and superheated, have been determined in recent years, and highly anomalous behavior has been found near the limiting temperatures in each case. For example, the heat capacities increase exponentially at each extreme. In the high temperature extreme this behavior is predictable from van der Waals theory, but the low temperature anomaly is not. The measurements will be reviewed, with emphasis on the more extensively studied super- (Continued) | | |

20.

cooled states at normal and high pressure, and evidence will be given that the low temperature anomalies can be described by expressions containing a singular temperature closely associated with the temperature of homogeneous nucleation of ice I.

| | |
|--------------------|--|
| Accession For | |
| NTIS GDA&I | <input checked="checked" type="checkbox"/> |
| DDC TAB | <input type="checkbox"/> |
| Unannounced | <input type="checkbox"/> |
| Justification | <i>for file</i> |
| By | <i>[signature]</i> |
| Distribution/ | |
| Availability Codes | |
| Dist | Avail and/or special |
| <i>A</i> | |

TABLE OF CONTENTS

| | |
|--|----|
| Abstract | 1 |
| Introduction | 1 |
| Measurement of Physical Properties in Metastable Regions | 4 |
| Physical Properties of Metastable Water | 5 |
| Superheated Region | 5 |
| Direct Measurement: Sound Velocity and Adiabatic Compressibility . | 5 |
| Extrapolated Properties | 7 |
| Supercooled Region | 10 |
| Thermodynamic Properties | 10 |
| Mass Transport Properties | 19 |
| Structure-Related Spectroscopic Studies | 25 |
| Discussion | 25 |
| Summary | 31 |
| Acknowledgements | 31 |
| References | 32 |
| Distribution List | 35 |

SUPERCOOLED AND SUPERHEATED WATER

C. A. Angell
Department of Chemistry
Purdue University
West Lafayette, Indiana 47907

ABSTRACT

Various thermodynamic, transport and structural features of water in its metastable states, both supercooled and superheated, have been determined in recent years, and highly anomalous behavior has been found near the limiting temperatures in each case. For example, the heat capacities increase exponentially at each extreme. In the high temperature extreme this behavior is predictable from van der Waals theory, but the low temperature anomaly is not. The measurements will be reviewed, with emphasis on the more extensively studied supercooled states at normal and high pressure, and evidence will be given that the low temperature anomalies can be described by expressions containing a singular temperature closely associated with the temperature of homogeneous nucleation of ice I.

INTRODUCTION

In comparison with the long-standing and intensive investigations of the properties of water in its thermodynamically stable states, the interesting extensions above the normal boiling point and below the normal freezing point have been more or less neglected. Although Kaemtz⁽¹⁾ measured the vapor pressure of water at -19°C in 1820 and Regnault⁽²⁾ extended the measurements to -32.8°C in 1847, there has been a surprisingly low level of interest in extending and improving the extent of knowledge of the physical properties

of water in this region. Even less effort has been devoted to characterizing water under superheated conditions, although the general pattern of behavior can be determined from measurements made at pressures above the saturated vapor pressure using short extrapolations to lower pressures.

Much more effort has been devoted to determining the limits of supercooling and superheating, particularly the former which is of special interest in relation to the initiation of raindrops by destabilization of clouds of supercooled water droplets. Thus it has been known since the time of Dufour, 1861, that small drops of clean water isolated from solid surfaces by suspension between layers of immiscible liquids, can be supercooled consistently to at least -34°C .⁽³⁾ More recently meteorologists, producing myriads of small, ($\sim 1\text{ }\mu\text{m}$) absolutely clean, water droplets in cloud chambers have determined that there is a rather sharply defined limiting range of -41 to -42°C in which $\sim 90\%$ of droplets in a given sample will freeze within a period of seconds.^(4, 5, 6) It is assumed that this limit is determined by a process of spontaneous order fluctuations intrinsic to the pure liquid phase, as distinct from the heterogeneous process, initiated on contaminant solid surfaces, by which liquids normally crystallize. It therefore sets the limit on the temperature range over which we can hope to determine the physical properties of liquid water, at least by measurements conducted on normal time scales.

In the superheated region, in which there is considerable technological interest because of explosion hazards in power plant heat exchangers, determinations of limiting temperatures have been made by a number of workers.⁽⁷⁻¹⁰⁾ These have usually been based on observations of spontaneous rupture of small water droplets rising in liquid columns through a temperature gradient. In the

most successful studies, water droplets of $\sim 10 \mu\text{m}$ diam. have been observed to reach a temperature of 279.5°C at 1 atm pressure before explosive vaporization occurs. (9,10)

In contrast with the case of supercooling the limit on superheating can be approximately predicted from equations of state, which imply the existence of regions of mechanical instability in which neither superheated liquid nor supercooled vapor can exist. For instance, a van der Waals equation with parameters based on critical point data⁽¹¹⁾ predicts the behavior shown by the set of isobaric T-V plots in Fig. 1. The maxima correspond to minima in the corresponding P-V isotherms, hence to points at which the liquid becomes mechanically unstable and must spontaneously rupture. The maximum

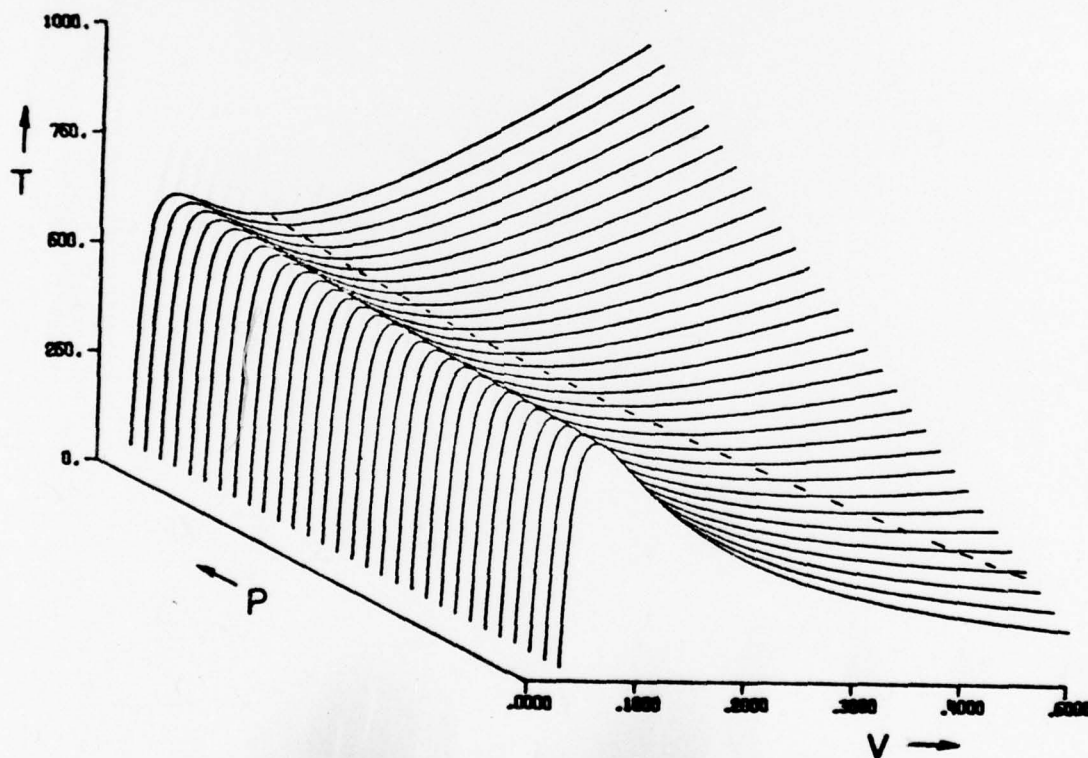


Fig. 1. V, T, isobars for water in the van der Waals approximation showing variation with pressure of spinodal points at limit of superheating of liquid and supercooling of vapor.

predicted for the 1 atm pressure isobar is 277°C very close to the observed superheating limit. Of course the van der Waals equation is inadequate to describe water and the observed limit must correspond to the kinetically controlled reflection of the true stability limit which would be located a little higher in temperature. In this region the instability must be anticipated by large fluctuations in density and entropy and these will be reflected in the magnitudes of the related thermodynamic properties, compressibility and heat capacity, which we will discuss below.

There is no corresponding accepted body of theory which predicts a mechanical stability limit for the supercooling temperature range for liquids, but the correspondences we will describe between liquid property anomalies in the two extreme ranges will suggest that the development of such a theory may be needed, at least for the case of water.

MEASUREMENT OF PHYSICAL PROPERTIES IN METASTABLE REGIONS

One of the reasons for the relative lack of information on metastable region properties is clearly the difficulty of maintaining the sample under study in the (thermodynamically unstable) liquid state during any measurement. Obtaining data under these conditions requires the development of special techniques. As implied in the previous section, the transition to the stable state can be impeded by removing all sources of external surfaces which catalyze the transition to the stable state. For macroscopic samples this requires exhaustive cleaning procedures. For purely statistical reasons, however, much less demanding sample preparation procedures may suffice if very small samples are used. Use of small samples has been the principle on which most of the recent measurements of water properties under metastable conditions have been carried out.

There are three approaches to small sample preparation. One may use (a) very thin films (between plastic or glass sheets), for e.g., spectroscopic studies in strongly absorbing regions;^(13,14) (b) small diameter columns (in glass or plastic capillaries) for volumetric, diffusion, or ESR studies;⁽¹⁵⁻¹⁸⁾ (c) very short small diameter columns or droplets, e.g. for NMR, viscosity, heat capacity and some spectroscopic studies.⁽¹⁹⁻²³⁾ For each dimension made microscopic in the above series, a gain in limiting temperature is made for a sample of given intrinsic cleanliness. With droplets, short term measurements can be made down to -38°C at the low temperature and up to $\sim 270^{\circ}\text{C}$ in the high temperature region. Many important results have recently been obtained using the Rasmussen MacKenzie emulsification technique⁽²²⁾ in which water is dispersed in $\sim 3\text{ }\mu\text{m}$ droplets in heptane or (similar hydrocarbon) supersaturated with SPAN 65 (sorbitan tristearate).

The actual methods in which the small samples are utilized in each particular measurement will not be reviewed here for lack of space, and the reader is referred to the original literature cited in the following sections.

PHYSICAL PROPERTIES OF METASTABLE WATER

Superheated Region

DIRECT MEASUREMENT: SOUND VELOCITY AND ADIABATIC COMPRESSIBILITY

It appears that despite the number of attempts to determine the superheating limit, the only physical property directly measured under superheated conditions is the sound velocity. This has been studied by Trinh and Apfel⁽²⁴⁾ to $\sim 180^{\circ}\text{C}$, which is, however, far short of the limit at $\sim 280^{\circ}\text{C}$. The results at the highest temperature differ slightly from those of McDade et al obtained under saturation conditions,⁽²⁵⁾ but concur in the continued curvilinear decrease

in velocity from the maximum-reached 75°C. Data are shown in Fig. 2. From the sound velocity data and extrapolated density data the adiabatic compressibilities κ_s can be calculated.

$$\kappa_s = 1/v^2 \rho \quad (1)$$

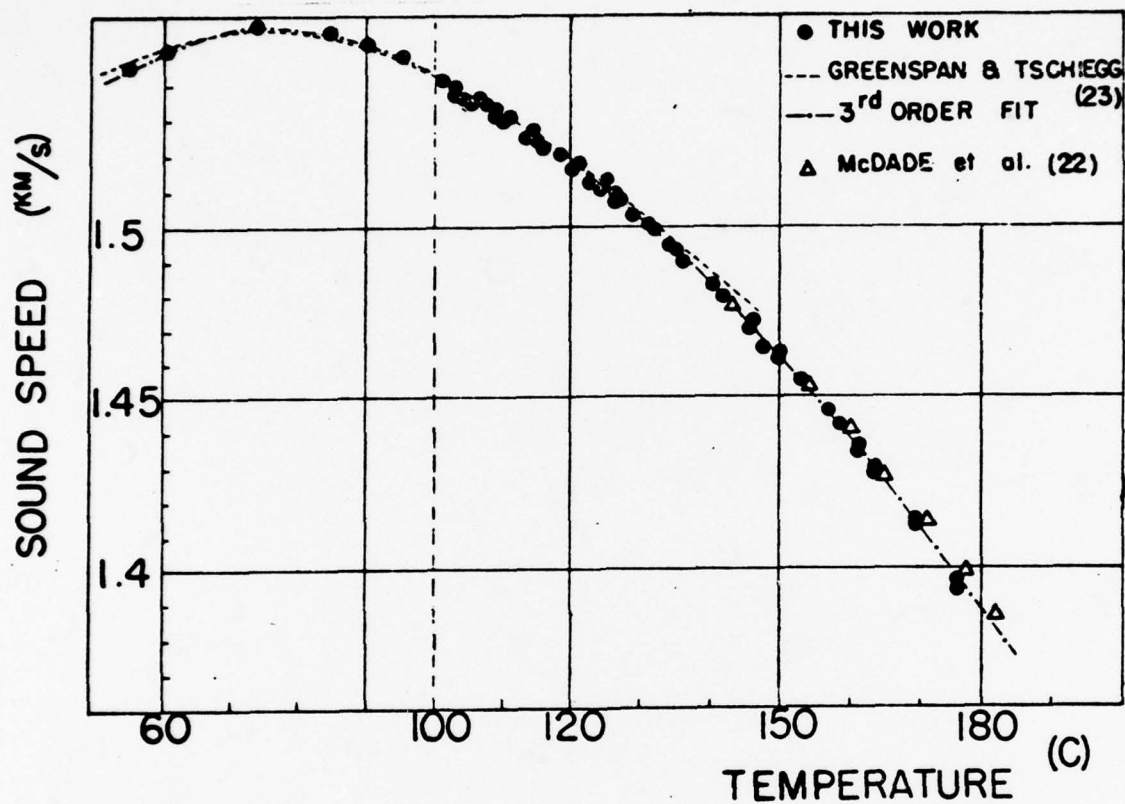


Fig. 2. Sound velocity in superheated water according to Trinh and Apfel (1978).

These are compared with the isothermal compressibilities extrapolated by Kell and Whalley⁽²⁶⁾ in Table 1 which is taken from Ref. 24.

TABLE 1 Thermodynamic parameters of superheated water under atmospheric pressure (after Trinh and Apfel (1978)).

| T (°C) | ρ (g/cm ³) | c (m/sec) | $\beta_s \times 10^{11}$ (cm ² /dyne) | $\beta_T \times 10^{11}$ (cm ² /dyne) | γ |
|-----------|--------------------------------|--------------|---|---|----------|
| 110 | 0.9509 | 1,532 | 4.45 | 5.08 | 1.142 |
| 120 | 0.9428 | 1,518 | 4.60 | 5.31 | 1.154 |
| 130 | 0.9344 | 1,501 | 4.75 | 5.57 | 1.172 |
| 140 | 0.9256 | 1,482 | 4.92 | 4.87 | 1.193 |
| 150 | 0.9165 | 1,460 | 5.11 | 6.21 | 1.215 |
| 160 | 0.9070 | 1,437 | 5.34 | | |
| 170 | 0.8968 | 1,412 | 5.59 | | |

EXTRAPOLATED PROPERTIES

Since accurate measurements of physical properties can be made at the saturation vapor pressure and at higher pressures, and since the saturation vapor pressure does not exceed even 10 atm before 180°C, many properties of superheated water at 1 atm pressure can be estimated quite accurately by short extrapolations vs. pressure. Such extrapolations have been made to 150°C by Kell and Whalley for the specific volume, using data of their own and of other authors as described in their definitive paper, ref. 26. Data at 0 and 10 bar (0.1 MPa) applied pressure are reproduced in Table 2.

TABLE 2 Specific volume of superheated water to 150°C, (Kell and Whalley, 1965)

| T | Density | |
|-----|-------------|------------|
| | 0.01 MPa | 0.1 MPa |
| 100 | 1.043451 | 1.042992 |
| 110 | 1.051594 | 1.051114 |
| 120 | 1.060364 | 1.059858 |
| 130 | 1.069791 | 1.069256 |
| 140 | 1.079900 | 1.079331 |
| 150 | 1.090735 | 1.090126 |

A method for estimating the specific heat of water for temperatures outside the stable region has been described by Lienhard⁽²⁷⁾ who derives the expression

$$C_p(T_r, p_r) = C_{p_{\text{ref}}} + \frac{0.001644 (1 - 1.2 p_r^2)}{(T_{r_m} - T_r)^{1/3}} \quad (2)$$

where $T_r = T/T_c$, T_c the critical temperature (= 647.2 K)

$p_r = p/p_c$, p_c the critical pressure (= 217.7 atm)

$C_{p_{\text{ref}}}$ = is the heat capacity at arbitrarily chosen reference pressure, e.g. 200 atm

T_{r_m} = the maximum superheating temperature at p_r .

Using the ASME Steam Table data for C_p at the reference pressure and taking T_{r_m} at 279.5°C, Eq. (2) yields the behavior shown in Fig. 3. The plot is presumably in error at the high temperature extreme because the spinodal at 1 atm pressure, where $C_p \rightarrow \infty$, will exceed the measured superheating limit 279.5°C by a short but unknown interval. The full curves show the predicted C_p for the case $T_{r_m} = 290$ and 299 K.

In either case the exponential increase in C_p , as the superheating limit of 279.5°C is approached, is striking and should be borne in mind in considering the observations on supercooled water in the following section.

Superheated water has been observed recently at temperatures as low as -18°C by Henderson and Speedy,⁽²⁸⁾ using a technique which places small samples of water confined in capillaries under isotropic tension. Superheated water at a pressure of -118 bar (-1.18 MPa) has a density maximum at 6.1°C rising to 6.7°C at -156 bar. At the lower temperatures of their study, the water sample was simultaneously superheated and supercooled.

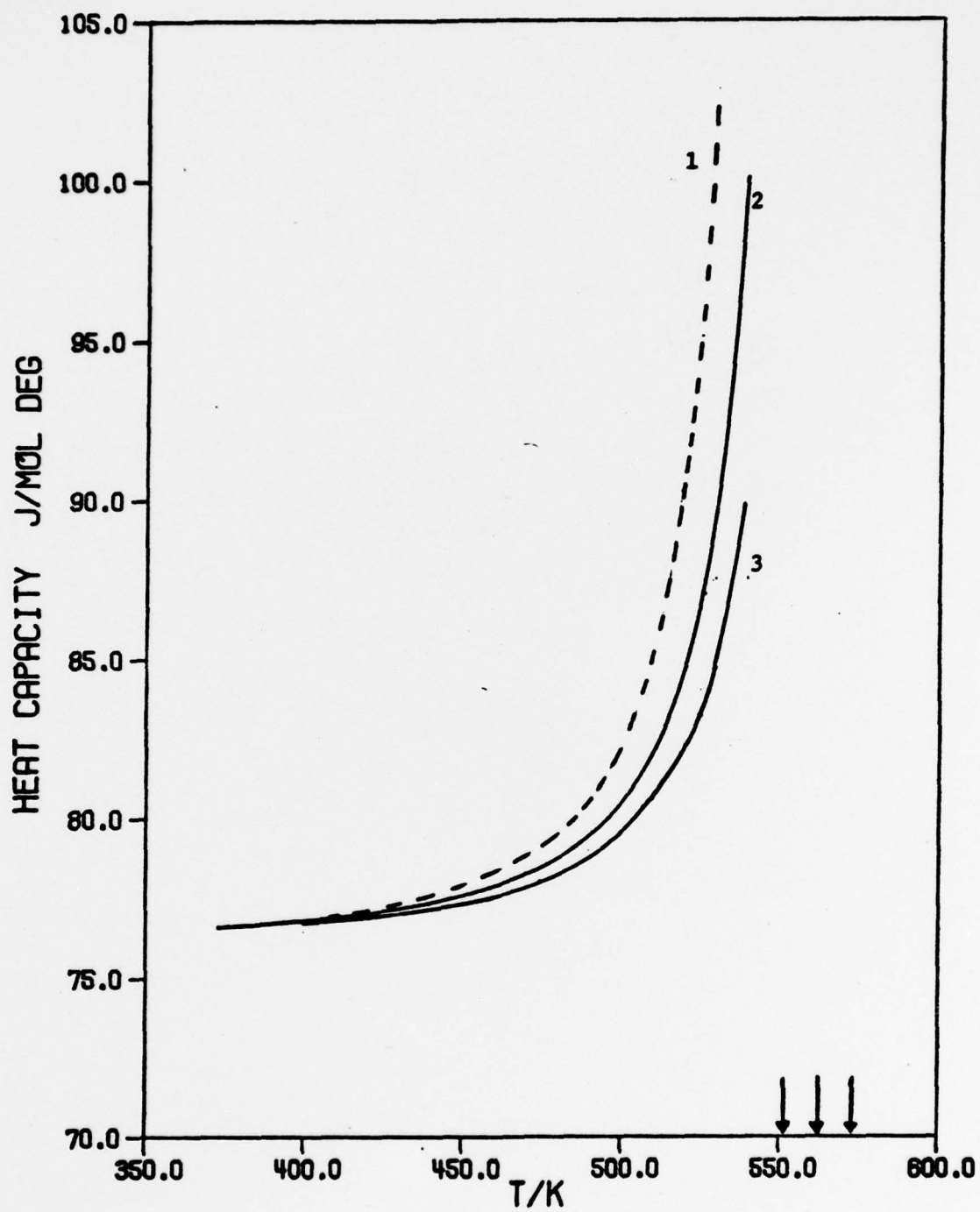


Fig. 3. Heat capacity of superheated water at one atm pressure from Eq. (2) with T_{r_m} (spinodal) taken to be either 279.5 (curve 1), 290 (curve 2) or 300 (curve 3).

Supercooled Region

THERMODYNAMIC PROPERTIES

The thermodynamic property which has been measured over the widest temperature range at normal pressure, and which now has been measured with perhaps the greatest accuracy, is the constant pressure heat capacity. It is probably true, also that the behavior of this fundamental property of water is the most immediately surprising of the many unusual aspects of the low temperature regime for this liquid, so it is appropriate to present these results first in this article.

Though known since 1890 to -5°C (Martinetti), the heat capacity was only shown to be highly unusual in the supercooled state by the emulsion measurements of Rasmussen et al⁽²⁹⁾ which extended to -38°C . These authors presented data from both differential scanning calorimetry and drift calorimetry, but the measurements were preliminary and not of great accuracy. There has been some effort recently in the author's laboratory to improve the accuracy and precision of this measurement. Using the Perkin Elmer DSC-2 differential scanning calorimeter, sets of data have been obtained by different operators, using different emulsification, calibration, and water content-determining procedures, which are self-consistent to $\pm 2\%$.⁽³⁰⁾ These data are presented in Table 3 and Figure 4. Some data at higher pressures have been derived by Kanno and Angell⁽³¹⁾ from combination of the Table 3 data, and high pressure volumetric results, discussed below, using the thermodynamic relation,

$$C_p(p) = C_p(0) - T \int_0^p \left(\frac{\partial^2 V}{\partial T^2} \right) dp \quad (3)$$

However, these are not considered of sufficient accuracy to present in tabular form.

TABLE 3 Heat capacity of supercooled water at one atm pressure

| t/°C | Specific Heat (J mole ⁻¹ deg ⁻¹) | |
|------|---|---------------------------|
| | Bulk Sample | Emulsion Sample (Average) |
| -3 | 75.7 | 76.0 |
| -8 | 76.6 | 76.2 |
| -13 | 77.6 | 77.4 |
| -18 | | 78.9 |
| -23 | | 81.4 |
| -28 | | 85.4 |
| -33 | | 92.7 |
| -35 | | 96.7 |

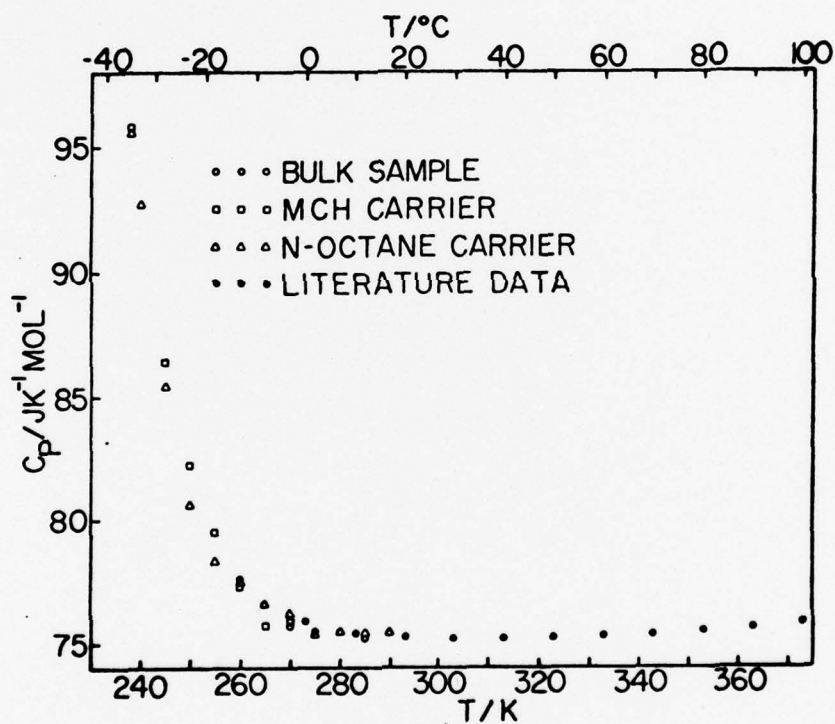


Fig. 4. Heat capacity of normal and supercooled water (from Angell, Oguni and Sichina (1979)).

Density measurements have been performed for H_2O and D_2O using both capillary column length measurements (by Schufle and coworkers^(32,33) and Zheleznyi⁽³⁴⁾) and emulsion volume measurements (by Rasmussen and MacKenzie⁽²²⁾) with results in good accord. Specific volumes and derived expansivities extend down to -34°C at one atmosphere pressure. These are presented in Table 4.

Table 4

Density, Molar Volume and Expansivity of H_2O and D_2O at One Atm Pressure

(after Zheleznyi, 1969)

| $t^\circ\text{C}$ | H_2O | | | D_2O | | |
|-------------------|--|--|--|--|--|--|
| | density ($\rho/\text{g cc}^{-1}$) | molar volume ($V/\text{cc mol}^{-1}$) | expansivity $10^4 \alpha/\text{deg}^{-1}$ | density ($\rho/\text{g cc}^{-1}$) | molar volume ($V/\text{cc mol}^{-1}$) | expansivity $10^4 \alpha/\text{deg}^{-1}$ |
| 0 | 0.9999 | 18.018 | | 1.1030 | 18.131 | |
| -5 | 0.9995 | 18.025 | - 1.7 | 1.1013 | 18.160 | - 4.12 |
| -10 | 0.9983 | 18.046 | - 3.1 | 1.0987 | 18.204 | - 5.9 |
| -15 | 0.9964 | 18.080 | - 4.7 | 1.0950 | 18.265 | - 8.5 |
| -20 | 0.9936 | 18.130 | - 7.0 | 1.0893 | 18.360 | -13.0 |
| -25 | 0.9895 | 18.206 | -10.8 | 1.0809 | 18.503 | |
| -30 | 0.9829 | 18.329 | -16.5 | | | |
| -34 | 0.9751 | 18.474 | | | | |

Using a high pressure capillary technique, these measurements have been extended to 190 MPa by Kanno and Angell,⁽³¹⁾ but only over a more limited temperature range and only for D_2O . Their data are shown in Table 5 which includes data from Kanno and Angell (1979) for normal pressure. Note how the temperature of the density maximum is depressed by increasing pressure.

Table 5

Specific Volume and Expansivity of D₂O Below 0°C and Above 1 atm Pressure

(Smoothed data, after Kanno and Angell)

P (applied pressure)

| t °C | 0 MPa | | 60 MPa | | 100.5 MPa | | 150.0 MPa | |
|------|------------------------------|-------------------------------------|-------------------------------|-------------------------------------|-----------------------------|-------------------------------------|----------------------|-------------------------------------|
| | V/cc g ⁻¹ | 10 ⁴ α/deg ⁻¹ | V/cc g ⁻¹ | 10 ⁴ α/deg ⁻¹ | V/cc g ⁻¹ | 10 ⁴ α/deg ⁻¹ | V/cc g ⁻¹ | 10 ⁴ α/deg ⁻¹ |
| 0 | 0.90523 | | 0.87870 | 0.2 ₆ | 0.86356 | | 0.84758 | |
| -3 | 0.90596 | -3.0 ₀ | 0.87869 | -0.1 ₅ | 0.86321 | 1.2 ₂ | 0.84694 | 2.4 ₀ |
| -5 | 0.90654 | -3.6 ₂ | 0.87875 | -0.4 ₉ | 0.86300 | 1.0 ₅ | 0.84654 | 2.3 ₀ |
| -7 | 0.90728 | -4.3 ₂ | 0.87886 | -0.8 ₁ | 0.86283 | 0.8 ₆ | 0.84616 | 2.2 ₀ |
| -10 | 0.90860 | -5.5 ₆ | 0.87914 | -1.3 ₄ | 0.86264 | 0.5 ₆ | 0.84563 | 2.0 ₆ |
| -12 | 0.90970 | -6.5 ₇ | 0.87942 | -1.7 ₅ | 0.86256 | 0.3 ₅ | 0.84530 | 1.9 ₅ |
| -15 | 0.91112 | -8.4 ₀ | 0.89980 | -2.5 ₀ | 0.86252 | 0.0 ₀ | 0.84484 | 1.8 ₀ |
| -17 | | | 0.88045 | -2.9 ₈ | 0.86255 | -0.2 ₆ | 0.84455 | 1.7 ₀ |
| -20 | | | | | 0.86266 | -0.6 ₅ | 0.84415 | 1.5 ₁ |
| -23 | | | | | 0.86288 | -0.9 ₂ | 0.84379 | 1.3 ₆ |
| -25 | | | | | 0.86308 | | 0.84356 | |
| | maximum density at 11.3°C | | maximum density at -1.85°C | | maximum density at -15°C | | | |

The high pressure data permit the assessment of isothermal compressibilities for D₂O. Data for supercooled water first obtained by Speedy and Angell to -26°C⁽³⁵⁾ are also available from a set of earlier measurements⁽¹⁵⁾ which were unsuitable for expansivity determinations. These are presented in Table 6 and Fig. 5.

Table 6
Isothermal Compressibilities of H₂O and D₂O
Below 0°C and Various Applied Pressures
(after Kanno and Angell (1980))

| t/°C | Isothermal Compressibility 10 ⁴ κ _T MPa ⁻¹ | | | | | | | |
|------|---|------------------|------------------|------------------|------------------|------------------|------------------|------------------|
| | H ₂ O | | | | D ₂ O | | | |
| | 0 | 50 MPa | 1000 MPa | 1500 MPa | 0 | 60 MPa | 1000 MPa | 1500 MPa |
| 0 | 5.0 ₉ | 4.4 ₂ | 3.8 ₅ | 3.4 ₄ | 5.4 ₀ | 4.5 ₆ | 4.0 ₂ | 3.4 ₉ |
| - 5 | 5.2 ₆ | 4.6 ₀ | 3.9 ₅ | 3.5 ₀ | 5.6 ₈ | 4.7 ₄ | 4.1 ₆ | 3.5 ₀ |
| -10 | 5.6 ₀ | 4.8 ₁ | 4.0 ₈ | 3.5 ₈ | 6.0 ₈ | 4.9 ₇ | 4.3 ₃ | 3.7 ₁ |
| -15 | 5.9 ₅ | 5.0 ₆ | 4.2 ₃ | 3.6 ₈ | 6.6 ₉ | 5.2 ₇ | 4.5 ₅ | 3.8 ₆ |
| -20 | 6.4 ₀ | 5.3 ₇ | 4.4 ₁ | 3.7 ₉ | 7.5 ₈ | 5.6 ₆ | 4.8 ₂ | 4.0 ₃ |
| -25 | | 5.7 ₅ | 4.6 ₂ | 3.9 ₁ | 8.9 ₀ | 6.2 ₄ | 5.1 ₇ | 4.2 ₅ |
| -30 | | | 4.8 ₇ | | | | | |

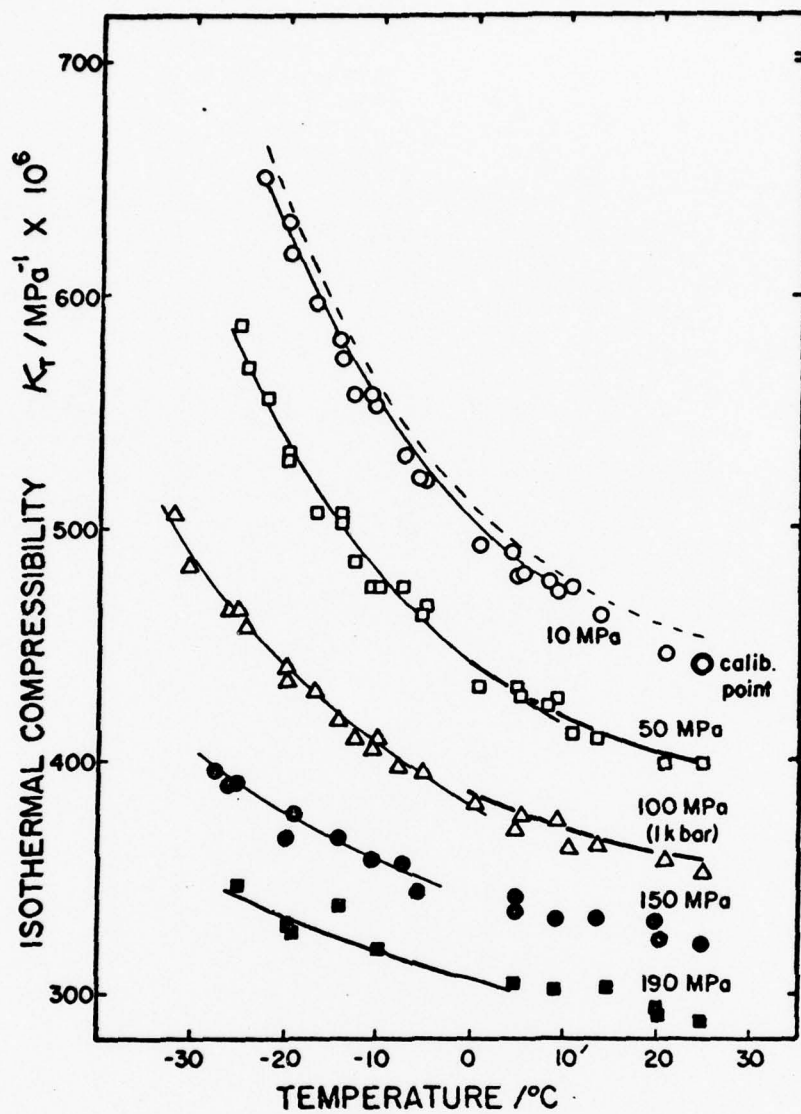


Fig. 5. Isothermal compressibilities of water at normal and high pressures, from Kanno and Angell (1979).

Adiabatic compressibilities may be calculated from the above data using the relation

$$\kappa_s = \kappa_T C_v / C_p = \kappa_T - \frac{\alpha^2 VT}{C_p} \quad (4)$$

or obtained directly from sound velocity measurements. The latter have been obtained by several groups working with different techniques in both ultrasonic^(24,35) and hypersonic frequency ranges.^(36,37) In each frequency range there is essential agreement amongst different groups down to -15°C , but there is a persistent and strange difference between the ultrasonic data on the one hand, and the zero frequency (Eq. 4) and the hypersonic data on the other. Leyendekkers⁽³⁸⁾ has reviewed the area and concludes that the isentropic assumption central to the data analysis is inadequate in the case of ultrasonic pressure waves. Data are presented graphically in Fig. 6. Below -15°C there are real data discrepancies amongst different workers which remain to be resolved.

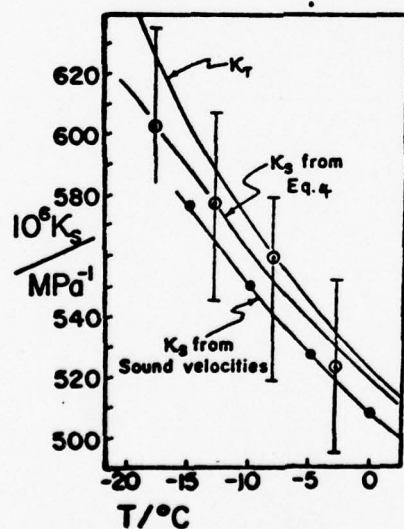


Fig. 6. Adiabatic compressibilities calculated from ultrasonic sound velocity measurements and from Eq. (4). At 0°C the latter value is accurately known, and the large uncertainties indicated by the error bars do not apply.

Vapor pressures in the supercooled states of water were first measured by Regnault in 1847 whose data extended to -32.8°C . Due to instrumental limitations these extraordinary measurements were not of great accuracy and are not quoted here. Scheel and Heuse⁽³⁹⁾ in 1909 obtained data to -15°C which have been confirmed recently by Bottomley.⁽⁴⁰⁾ A Van't Hoff plot of the data between 0 and -15°C is linear, and a vapor pressure of 1 mm Hg (13.3 Pa) is indicated at -20°C . Some data are given in Table 7.

Table 7

Vapor Pressure of Supercooled Water
(Data selection from Scheel and Heuse (1909))

| $t/^{\circ}\text{C}$ | p/mm |
|----------------------|---------------|
| - 2.814 | 3.724 |
| - 2.816 | 3.726 |
| - 2.830 | 3.726 |
| - 2.838 | 3.724 |
| - 3.918 | 3.432 |
| - 4.842 | 3.209 |
| - 4.884 | 3.202 |
| - 4.900 | 3.193 |
| - 7.250 | 2.675 |
| - 7.279 | 2.669 |
| - 7.301 | 2.665 |
| - 7.313 | 2.661 |
| - 8.804 | 2.373 |
| - 9.115 | 2.315 |
| - 9.812 | 2.191 |
| -15.176 | 1.421 |
| -15.308 | 1.412 |

The static dielectric constant (relative permittivity) of water below 0°C has been measured by Hasted and Shahidi⁽⁴¹⁾ using an absolute method based on dilute emulsion samples analyzed using the Maxwell-Lewin formula for the mean permittivity ϵ_m of a dispersion of spheres of a substance of dielectric constant ϵ_1 in a matrix of dielectric constant ϵ_2 . When the volume fraction of spheres is ϕ , the relation is

$$\epsilon_m = 3 \phi \epsilon_2 \left(\frac{\epsilon_1 - \epsilon_2}{2\epsilon_2 + \epsilon_1} \right) + \epsilon_2 \quad (5)$$

Their results, shown in Fig. 7, have been supported by independent measurements of Hodge and Angell⁽⁴²⁾ based on the Maxwell-Wagner effect for concentrated emulsions, using an analysis which requires calibration with known values at some reference temperature.

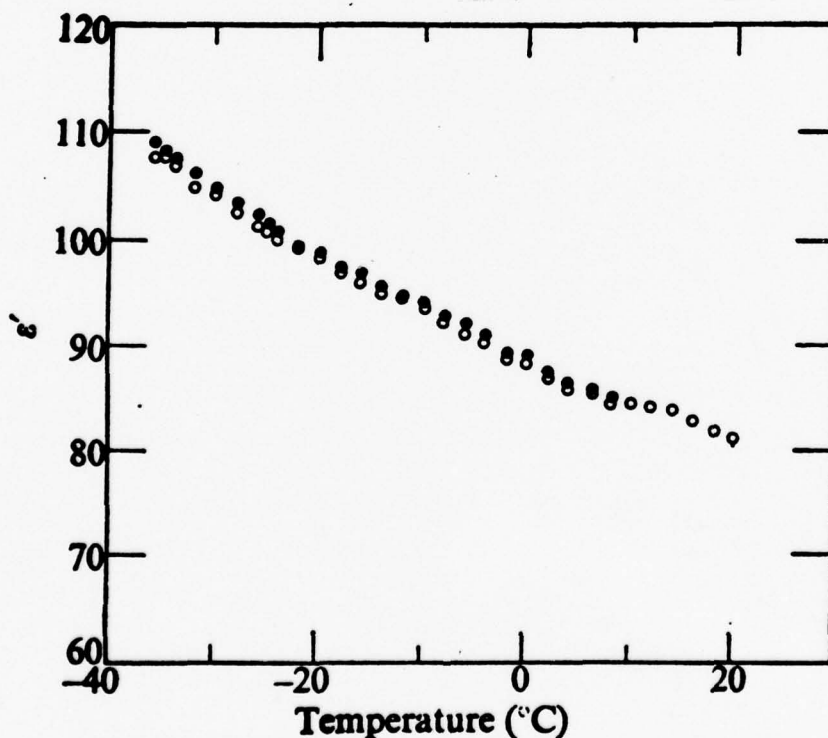


Fig. 7. Dielectric constant (relative permittivity) for supercooled water (after Hasted and Shahidi, ref. 41).

MASS TRANSPORT PROPERTIES

The intensive thermodynamic properties discussed above are determined by the magnitude of fluctuations in extensive properties which are characteristic of the liquid at equilibrium. The transport properties likewise are determined by the growth and decay rates of these same fluctuations, hence are in a sense also equilibrium properties of the liquid. However, they are almost invariably determined by deliberately perturbing the equilibrium state of the system and observing the rate of return to equilibrium, hence they are usually considered separately as "non-equilibrium" properties.

Fundamentally related to the process of recovery of equilibrium after most types of perturbation is the ordinary (mass) diffusion process. This has been studied in the supercooled range by Pruppacher⁽¹⁶⁾ using the classical radiotracer diffusion-out-of-capillary technique and reaching a surprising -25°C and by Gillen et al⁽¹⁷⁾ using the shorter time NMR spin-echo technique. The latter authors reached -31°C with groups of selected capillary sample containers. Attempts to extend these measurements to lower temperatures using pulsed gradient method on emulsion samples have only been partially successful.⁽⁴³⁾

Data from the preferred study of Gillen et al are presented in Table 8 after a uniform 6.7% upward correction to normalize to the accepted diaphragm method value for bulk water.⁽⁴⁴⁾

The viscosity of water was first measured below 0°C in 1913 by White and Twining⁽⁴⁵⁾ whose data penetrated to -14°C . Fifty years later Hallett⁽⁴⁶⁾ used a clever cold capillary method to extend the range to -24°C . Very recently Osipov et al⁽²¹⁾ have reached -35°C with a moving microscopic slug technique which gives results in agreement to 1% with those of Hallett in their

Table 8

Self-Diffusion Coefficients of Water
 Into the Supercooled Range
 (After Gillen, Douglass and Hoch (1972)
 normalized to Mills⁽⁴⁴⁾ datum at 25°C)

| $t^{\circ}\text{C}$ | $10^5 D/\text{cm}^2 \text{ sec}^{-1}$ |
|---------------------|---------------------------------------|
| 25.1 | 2.38 |
| 12.2 | 1.69 |
| 2.4 | 1.12 |
| - 9.4 | 0.75 |
| -11.6 | 0.675 |
| -14.4 | 0.590 |
| -17.3 | 0.509 |
| -19.1 | 0.467 |
| -21.3 | 0.421 |
| -23.1 | 0.364 |
| -24.9 | 0.343 |
| -26.8 | 0.281 |
| -28.7 | 0.234 |
| -30.6 | 0.200 |

common temperature range. With the latter data, viscosity becomes the most extensively studied transport property for water, though in the case of D_2O , the deuteron spin relaxation time data cover a wider equivalent range. The viscosity data collected in Table 9 are combined with the stable range data in an Arrhenius plot, Fig. 8, to demonstrate the extraordinary departures from Arrhenius behavior exhibited by water in this low temperature range. The apparent activation energy in the lowest temperature interval has risen to 14 kcal/mole (59 kJ/mole).

Table 9
Viscosity of Water Below 0°C

| $t/^{\circ}\text{C}$ | White & Twining (1913) | Hallett (1963) | Osipov and coworkers (1979) |
|----------------------|---------------------------|-------------------|--------------------------------|
| 0 | 1.798 | 1.79 | 1.80 |
| - 4.70 | 2.121 | | |
| - 5 | | 2.16 | 2.14 |
| - 7.23 | 2.341 | | |
| - 9.30 | 2.549 | | |
| -10 | | 2.66 | 2.60 |
| -15 | | 3.34 | 3.23 |
| -20 | | 4.33 | 4.36 |
| -25 | | | 6.45 |
| -30 | | | 10.2 |
| -32 | | | 12.7 |
| -34 | | | 16.4 |
| -35 | | | 18.7 |

The electrical conductivity of water, which proceeds by a proton-hopping (Grotthus) mechanism, has not been properly measured into the supercooled region. The dielectric relaxation time, which reflects the reorientation kinetics of the molecules and is described extraordinarily well by the simple Debye relaxation theory in the stable range, has only been measured to -8°C , where $\tau_D = 2.5 \times 10^{-11}$ s. ⁽⁴⁷⁾ According to the Debye model, in which τ_D scales with η/T , τ_D should grow to 1.4×10^{-10} by -35°C .

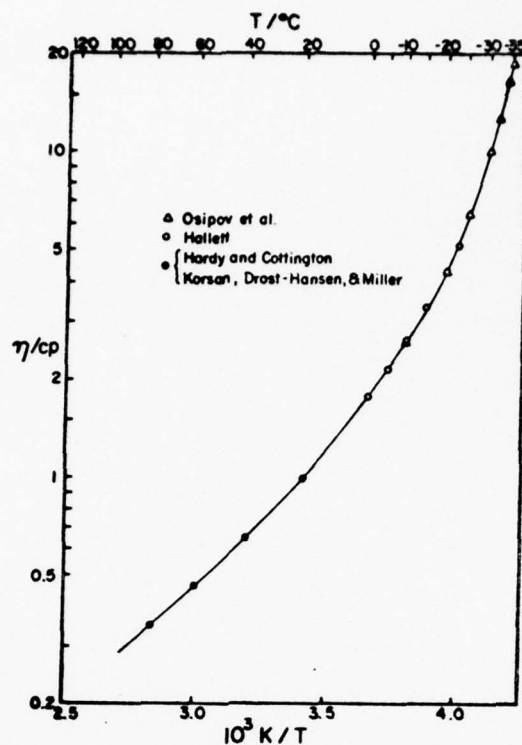


Fig. 8. Arrhenius plot of viscosity data for normal and supercooled water.

Nuclear spin relaxation times can be measured on very small and quiescent pure water samples and, with almost equal accuracy, on capillary or emulsion droplet samples, hence the data for these relaxation processes are very extensive. Hindman and coworkers^(19,49-50) have reported measurements down to -31°C for ^{17}O and ^1H relaxation (where instrumental electronic problems were limiting) and down to -36°C for ^2D in D_2O . An example of their results in which both bulk water and emulsion sample data are included is shown in Fig. 9. For the ^1H and most recently ^2D cases, our knowledge of nuclear spin relaxation processes has been extended most usefully to pressures of 250 MPa (2.5 kbar) and temperatures as low as -86°C by Lang and Lüdemann⁽²⁰⁾ using a

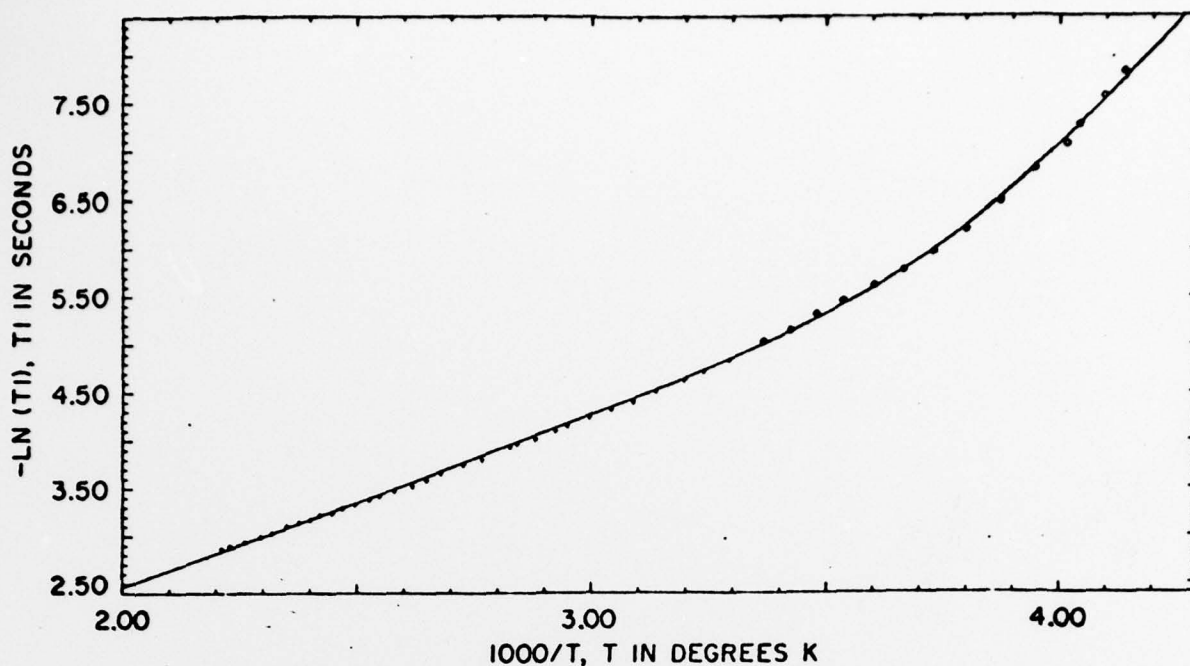


Fig. 9. Arrhenius plot of spin lattice relaxation time for ^{17}O in normal and supercooled water (after Hindman, ref. 50).

high pressure strengthened glass sample cell. Using a frequency of $\omega_0 = 6.28 \times 10^8$ Hz, these workers were able to observe a T_1 minimum (at -70°C , 200 MPa) hence were able to derive, from $\omega_0 \tau_\theta = 1$, a reorientation correlation time τ_θ of 1.6×10^{-9} sec, ~ 3 orders of magnitude longer than at 25°C . Water under these conditions is evidently a rather viscous liquid, with a viscosity of ~ 10 poise (c.f. glycerol under ambient conditions, $\eta = 15$ poise), if the Debye reorientation time theory continued to apply even approximately. Reorientation times derived for a range of conditions by Lang and Lüdemann are shown in Fig. 10. The temperature dependence of the reorientation time at high pressure proves to be distinct from that at 1 atm pressure and instead is

characteristic of that of any moderately viscous liquid, obeying the VTF equation

$$\tau = \tau_0 \exp - B/(T-T_0) \quad (6)$$

with parameters $\tau_0 = 3.13 \times 10^{-14}$ sec, $B = 749$ K and $T_0 = 127$ K, T_0 being appropriately (Angell and Tucker⁽⁵¹⁾), about 20° below the glass transition temperature estimated by short extrapolation of measured values in aqueous solutions at the same pressure. (52)

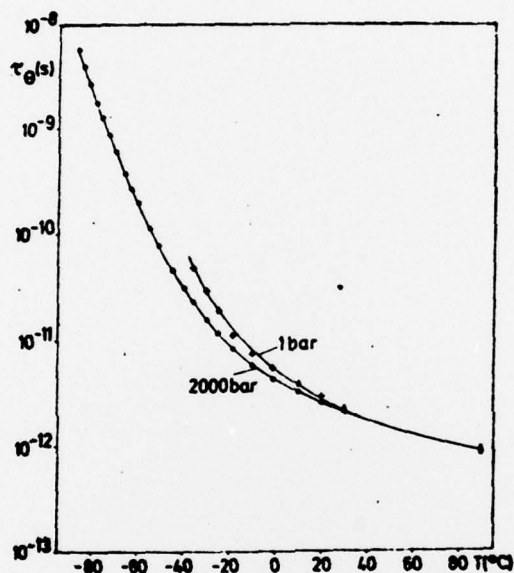


Fig. 10. Arrhenius plot of reorientation correlation times for water at 1 atm and 200 MPa (2 kbar) obtained from high pressure NMR data (after Lang and Lüdemann, ref. 20).

Reorientation times have been measured at one atmosphere pressure for dilute radical solute species in water at temperatures down to -33°C , by ESR measurements. Ahn⁽¹⁸⁾ showed that the reorientation time for ditertiary butyl nitroxide at concentrations of 10^{-4}M followed the viscosity temperature dependence down to -24°C , and successfully predicted the then unknown viscosity of water at -33°C .

STRUCTURE-RELATED SPECTROSCOPIC STUDIES

Several spectroscopic studies have been performed on water in the supercooled state, and others are in progress. NMR chemical shift measurements which average overall configurations, and infra-red measurements, which are "seeing" a much shorter time scale structure, have been studied to -35°C ,^(23,53) but these results are not discussed here (see original literature and review by the author in "Water: A Comprehensive Treatise," Vol. 7 (Ed. F. Franks, 1980)).

DISCUSSION

The results reviewed above offer a very demanding challenge to the theoretician.

The rapid variation in thermodynamic properties at low temperatures, which are so similar to that of the heat capacity at high temperature (compare Figs. 3 and 4), suggests the possibility at low temperature of a thermodynamic singularity analogous to the instability (spinodal) point at high temperatures described in the introduction. This possibility is strengthened when the data are plotted against the familiar critical point temperature function $\epsilon = (T - T_s)/T_s$ where T_s is the singular or spinodal point.⁽³⁵⁾ This is shown for two properties, the expansivity α (a thermodynamic property) and the viscosity η , (a transport property) in Fig. 11. For α , a small, linearly

temperature-dependent, component has first been subtracted in order that the component being plotted does not become zero at any temperature. This linear component represents the "normal" (non-critical or non-anomalous) part of the thermodynamic property, which is always superimposed on the anomalous part in any static property of the system. Such a subtraction need not be made in the case of the viscosity because the shear relaxation time is dominated by the decay time of the anomalous fluctuations. Both properties give linear plots when T_s is fixed at 228 K. Currently, attempts are being made to derive, from binary solution studies in which the anomalous behavior at low temperatures is eliminated, appropriate background ("normal") components for the heat capacity and isothermal compressibility (Angell and Tucker,⁽⁵⁴⁾ Oguni and Angell⁽⁵⁵⁾) so that the exponents describing the singular part can be determined.

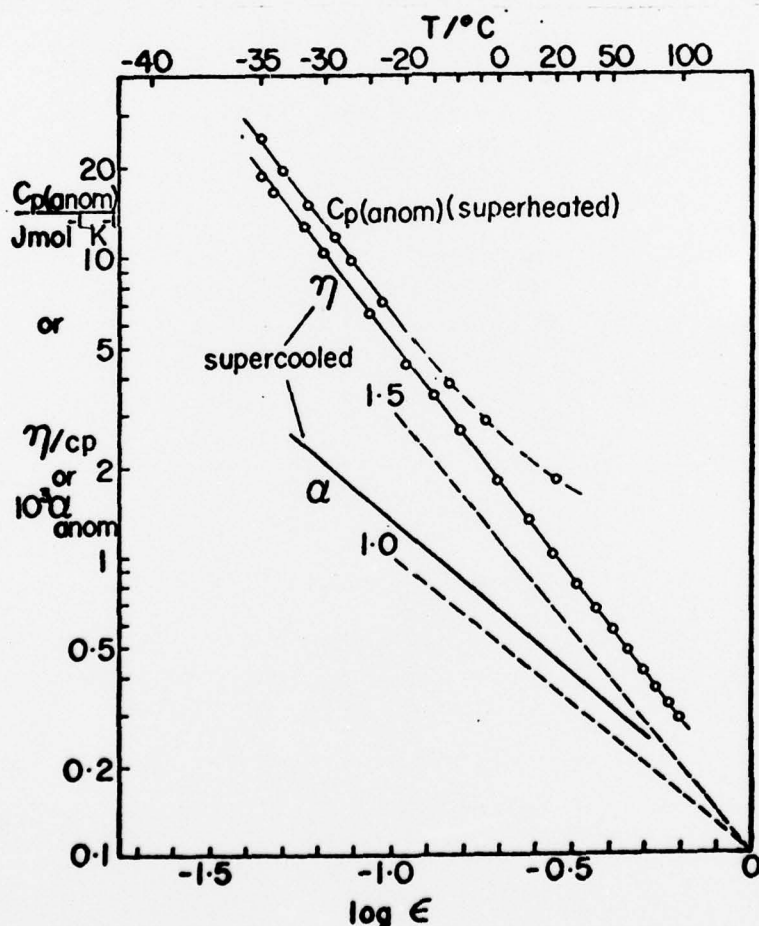


Fig. 11. Plot of anomalous components of selected supercooled and superheated water thermodynamic properties, and of viscosity for supercooled water vs $\log (T/T_s - 1)$ with $T_s = 228$ K.

It is to be noted that 228 K is only some 5 K below the lowest temperature T_H , to which small samples can be supercooled before crystallization occurs. This suggests strongly that the singular point is indeed a low temperature mechanical stability limit for the liquid phase analogous to that for the superheated liquid discussed earlier, although "internal" liquid phase interpretations of T_g are also possible.

It is unfortunate that no directly measured high temperature data near the high temperature T_g are available to include for comparison with the supercooled water data. In their absence, we use the Eq. (2) - based data displayed in Fig. 3, after subtracting a constant "background" (normal component) of $75 \text{ J mol}^{-1} \text{ deg}^{-1}$, to obtain the plot labelled C_p (superheated) in Fig. 11. The data at large ϵ (where the anomalous component should become dominant, and the error in choice of background be least influential) are linear in ϵ with a slope of 1.5. This, however, is larger than the expected classical value 1.0, and larger than even the lattice gas value, 1.25, which might be expected to apply very near the spinodal if measurements were possible. It is probable that, close to T_g , the form of Eq. (2) becomes inadequate. If we take T_g at the high temperature limit to be 300°C , then at 279.5°C where spontaneous rupture is observed, the value of ϵ is almost the same as that of supercooled water at -40°C where homogeneous nucleation of similar size droplets is observed.

Considering the low temperature behavior further, Kanno and Angell⁽¹⁵⁾ have shown that the close relation between T_H and T_g is maintained as pressure is increased to 200 MPa even though T_H decreases by more than 50 K (to -92 K at 200 MPa). On the other hand, both thermodynamic and relaxation time data at pressure above 200 MPa indicate⁽¹⁵⁾ the disappearance of

singular behavior (T_g becomes too low) and the return to "normal" low temperature liquid behavior in which the temperature T_0 appears as some kind of internal equilibrium low temperature limit on the liquid; in effect, a temperature at (or before) which it would undergo a second (or higher) order transition to an "ideal glass" phase.⁽⁵⁶⁻⁵⁹⁾ In practice liquids always pass, for kinetic reasons, through a non-equilibrium transition (the "glass transition") at some temperature T_g a little higher than T_0 . (So far, not even the glass transition has been observed for water because of fast crystallization even in the region above 200 MPa, though several attempts have been made in the author's laboratory to suppress the latter by fast quenching procedures).

The above observations on the thermodynamic characterization of water are summarized in Fig. 12 in the form of a qualitative, but realistically

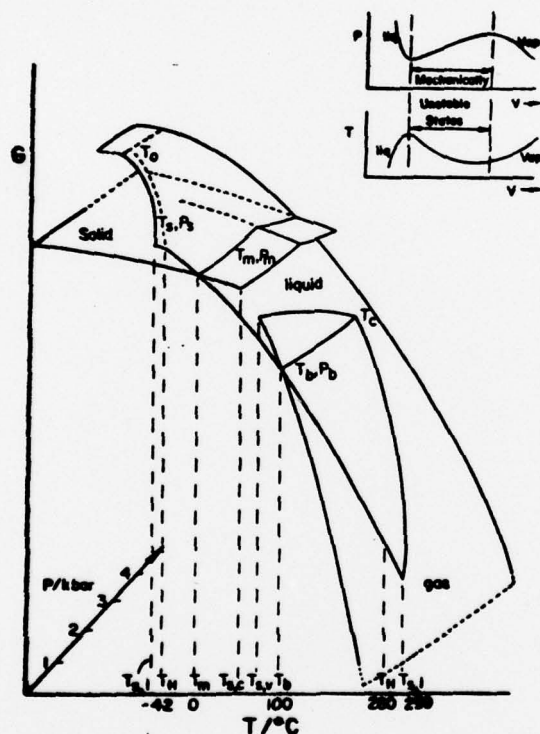


Fig. 12. Free energy surfaces for solid, liquid and gaseous phases of water showing metastable surfaces and their stability edges, as described in text.

scaled, free energy surface diagram for water. This shows the intersections with stable crystal polymorph and gas free energy surfaces which give us the normal crystallization and boiling phenomena, but also

(a) the metastable extensions of the liquid and gas surfaces at

$T < T_c$, $P < P_c$, showing the surface edges corresponding to mechanical stability limits on vapor supercooling $T_{s,v}$ and liquid superheating $T_{s,l}$;

(b) the metastable extensions of crystal and liquid surfaces

showing a (necessary but unobservable) superheating limit $T_{s,c}$ for the crystal due to shear mode instabilities at an unknown high temperature, and the putative mechanical stability limit on liquid supercooling $T_{s,l}$;

(c) the vanishing, at higher pressures, of the low T instability edge

as $T_{s,l}$ falls below T_0 . In the higher pressures the amorphous phase surface is seen, ideally, as continuing to 0 K with a slope discontinuity at T_0 such that below T_0 the surface has essentially the same temperature derivative (i.e. entropy) as the stable crystalline phase at that temperature.

Providing a theoretical basis for the impending low temperature catastrophe is a somewhat difficult problem, particularly as there are no other examples of liquids exhibiting this type of behavior known at this time. The facts that

(i) the anomalies are suppressed by constraining the system to constant volume (C_v actually decreases slightly with decreasing temperature in the temperature range 0 to -40°C ⁽⁵³⁾), and

(11) the anomalies are banished even from constant pressure properties at high pressures where the water molecules are forced into closer packing arrangements,

imply that geometrical aspects of the packing of water molecules in the preferred open tetrahedral network configuration are of central importance. Two theoretical approaches consistent with this observation are currently under development. One, due to Stanley and Teixeira^(60,61) is basically a theory of gelation of fully bonded (hence open-packed) water molecules, in which a percolation threshold near -45°C appears to arise as a natural consequence of the random formation of hydrogen bonds of fixed energy. The other, by Stillinger⁽⁶²⁾ is a more general development of the statistical mechanics of finite systems in which the differential geometry of a configuration space surface seems to lead naturally to a catastrophe at sufficient supercooling.

These ideas are yet at an early stage of their development and the appropriate role played in the phenomenology by cooperative hydrogen bonding (i.e. energetic factors as opposed to purely geometrical factors) imposing a superstructure of consequences on a framework of random hydrogen bonding remains to clearly delineated. It is certain, however, that from a successful treatment of the supercooled water phenomenology there will emerge a much more complete and sophisticated picture of the nature of liquid water than is currently available.

SUMMARY

A review of recent measurements and calculations on properties of water in metastable superheated and supercooled states shows the existence of interesting parallels in behavior which are probably unique to pure water at relatively low pressure (~ 200 MPa). For this case the singular behavior expected for all liquids at large superheating, as they approach their mechanical stability limits, is repeated in the low temperature supercooled regime. Available data are consistent with a singular temperature of 228 K, at 1 atm. More accurate and more extensive data are needed to elucidate this behavior. The singular behavior is eliminated by sufficient increases in applied pressure, as the hydrogen bond angle relationships essential to the manifestation of the singularity, are suppressed.

ACKNOWLEDGEMENTS

The author is indebted to the Office of Naval Research for support of this work under Project No. N00014-78-C-0035. He is also grateful to a number of colleagues, F. H. Stillinger, H. E. Stanley, M. Oguni, W. Sichina, H. Kanno, and R. J. Speedy, for allowing him to see and discuss data and ideas not currently in print.

REFERENCES

1. W. Kaentz, *Traité de Météorologie*, I, 290 (1820).
2. V. Regnault, *Annales de Chemie et de Physique*, 3e série XI, 273 (1844).
V. Regnault, *Memoires de L'Academic Royale des Sciences de Institute de France* XXI, 465 (1847).
3. L. Dufour, *Archives Sci. Phys. Nat.* 10, 364 (1861).
4. B. J. Mason, *Clouds, Rain and Rainmaking* (Cambridge: University Press) (1962).
5. D. G. Thomas and L. A. K. Staveley, *J. Chem. Soc.*, V, 4569 (1952).
6. R. J. Anderson and J. L. Kassner, to be published; R. J. Anderson, Ph.D. thesis, University of Missouri, Rolla, (1978).
7. V. Skripov, "Metastable Liquids"
8. J. G. Eberhart and H. C. Schnyders, *J. Phys. Chem.* 77, 2730 (1973).
9. R. E. Apfel, *Nature, Physical Science* 238, 63 (1972).
10. M. Blander, D. Hengstenberg and J. L. Katz, *J. Phys. Chem.*, 75, 3613, (1971).
11. For example, G. M. Barrow, "*Physical Chemistry*", McGraw Hill, lists
 $a = 5.464 \text{ atm } \ell^2 \text{ mole}^{-2}$ and $b = 0.0305 \ell \text{ mol}^{-1}$ obtained from $b = \frac{1}{3} V_c$
and $a = 3 P_c V_c^2$.
12. W. J. Sichina, Ph.D. Thesis, Purdue University, (1979).
13. P. A. Giguère and K. B. Harvey, *J. Mol. Spec.* 3, 36-35 (1959).
14. R. Barkatt and C. A. Angell (unpublished work).
15. H. Kanno and C. A. Angell, *J. Chem. Phys.* 70, 4008 (1979).
16. H. Pruppacher, *J. Chem. Phys.* 56, 101, (1972).
17. K. T. Gillen, D. C. Douglass and M. J. R. Hoch, *J. Chem. Phys.* 57, 5117 (1972).
18. M. -K. Ahn, *J. Chem. Phys.* 64, 134, (1976).
19. J. C. Hindman and A. Svirnickas, *J. Phys. Chem.* 77, 2487, (1973).

REFERENCES (Cont.)

20. E. Lang and H. -D. Lüdemann, J. Chem. Phys. 67, 718 (1977).
21. Yu. A. Osipov, B. V. Zheleznyi, and N. F. Bondarenko, Transl. Zhur. Fiz. Khim. 51, 1264 (1977).
22. D. H. Rasmussen and A. P. MacKenzie, J. Chem. Phys. 59, 5003 (1973).
23. C. A. Angell and V. E. Rodgers (to be published).
24. E. Trinh and R. E. Apfel, J. Chem. Phys. 69, 4245 (1978); J. Acoust. Soc. Am. 63, 777 (1978).
25. J. McDade, D. Pardue, A. Hedrich and F. Vrataric, J. Acoust. Soc. Am. 31, 1380 (1959).
26. G. S. Kell and E. Whalley, Philos. Trans. R. Soc. Lond. Ser. A258, 565 (1965).
27. J. H. Lienhard, Nucl. Sci. Eng. 62, 302 (1977).
28. S. J. Henderson and R. J. Speedy, J. Sci. Inst. (submitted 1979).
29. D. H. Rasmussen, A. P. MacKenzie, J. C. Tucker and C. A. Angell, Science 181, 342 (1973).
30. C. A. Angell, M. Oguni and W. J. Sichina (submitted to Science, 1979).
31. H. Kanno and C. A. Angell, J. Chem. Phys. (submitted (1979)).
32. J. A. Schufle, Chem. Ind. 16, 690 (1965).
33. J. A. Schufle and M. Venugopalan, J. Geophys. Res. 72, 3271 (1967).
34. B. V. Zheleznyi, Russ. J. Phys. Chem. 42, 950 (1968); 43, 1311 (1969).
35. R. J. Speedy and C. A. Angell, J. Chem. Phys. 65, 851 (1976).
36. J. Rouch, C. C. Lai, and S. H. Chen, J. Chem. Phys. 65, 4016, (1976); 66, 5031 (1977).
37. J. Teixeira and J. Leblond, J. de Physique, Lett. 39, L83 (1978).
38. J. V. Leyendekkers, J. Phys. Chem. 83, 347 (1979).
39. K. Scheel and W. Heuse, Ann. Physik 29, 763 (1909).
40. G. A. Bottomley, Aust. J. Chem. 31, 1177 (1978).
41. J. B. Hasted and M. Shahidi, Nature, 262, 777 (1976).

REFERENCES (Cont.)

42. I. M. Hodge and C. A. Angell, J. Chem. Phys. 68, 1363 (1978).
43. C. A. Angell, E. D. Finch and P. Bach (unpublished work).
44. R. Mills, J. Phys. Chem. 77, 685 (1973).
45. G. F. White and R. W. Twining, Amer. Chem. J. 50, 380 (1913).
46. J. Hallett, Proc. Phys. Soc. 82, 1046 (1963).
47. J. A. Saxton and J. A. Lane, Proc. Roy. Soc. A 213, 400 (1952).
48. J. C. Hindman, A. J. Zielen, A. Svirmickas, and M. Wood, J. Chem. Phys. 54, 621 (1971).
49. J. C. Hindman, A. Svirmickas, and M. Wood, J. Phys. Chem. 74, 1266 (1970); J. Chem. Phys. 59, 1517 (1972).
50. J. C. Hindman, J. Chem. Phys. 60, 4488 (1974).
51. C. A. Angell and J. C. Tucker, J. Phys. Chem. 78, 278 (1974).
52. H. Kanno and C. A. Angell, J. Phys. Chem. 81, 2639 (1977).
53. C. A. Angell, J. Shuppert and J. C. Tucker, J. Phys. Chem. 77, 3092 (1973).
54. C. A. Angell and J. C. Tucker
55. M. Oguni and C. A. Angell (to be published).
56. J. H. Gibbs and E. A. Dimarzio, J. Chem. Phys. 28, 373 (1958).
57. M. Goldstein, J. Chem. Phys. 67, 2246 (1977).
58. C. A. Angell and K. J. Rao, J. Chem. Phys. 57, 470 (1972).
59. M. H. Cohen and G. S. Grest, Phys. Rev. B, 20, 1077 (1979).
60. H. E. Stanley, J. of Phys. A, 12 (in press).
61. H. E. Stanley and J. Teixeira (to be published).
62. F. H. Stillinger, Am. Chem. Soc. Symposium Series, Ed. Stanley P. Rowland (to be published).

TECHNICAL REPORT DISTRIBUTION LIST, GEN

| | <u>No. Copies</u> | | <u>No. Copies</u> |
|--|-----------------------|--|-----------------------|
| Office of Naval Research 800 North Quincy Street Arlington, Virginia 22217 Attn: Code 472 | 2 | Defense Documentation Center Building 5, Cameron Station Alexandria, Virginia 22314 | 12 |
| ONR Branch Office 536 S. Clark Street Chicago, Illinois 60605 Attn: Dr. George Sandoz | 1 | U.S. Army Research Office P.O. Box 1211 Research Triangle Park, N.C. 27709 Attn: CRD-AA-IP | 1 |
| ONR Branch Office 715 Broadway New York, New York 10003 Attn: Scientific Dept. | 1 | Naval Ocean Systems Center San Diego, California 92152 Attn: Mr. Joe McCartney | 1 |
| ONR Branch Office 1030 East Green Street Pasadena, California 91106 Attn: Dr. R. J. Marcus | 1 | Naval Weapons Center China Lake, California 93555 Attn: Dr. A. B. Amster Chemistry Division | 1 |
| ONR Area Office One Hallidie Plaza, Suite 601 San Francisco, California 94102 Attn: Dr. P. A. Miller | 1 | Naval Civil Engineering Laboratory Port Hueneme, California 93401 Attn: Dr. R. W. Drisko | 1 |
| ONR Branch Office Building 114, Section D 666 Summer Street Boston, Massachusetts 02210 Attn: Dr. L. H. Peebles | 1 | Professor K. E. Woehler Department of Physics & Chemistry Naval Postgraduate School Monterey, California 93940 | 1 |
| Director, Naval Research Laboratory Washington, D.C. 20390 Attn: Code 6100 | 1 | Dr. A. L. Slafkosky Scientific Advisor Commandant of the Marine Corps (Code RD-1) Washington, D.C. 20380 | 1 |
| The Assistant Secretary of the Navy (R,E&S) Department of the Navy Room 4E736, Pentagon Washington, D.C. 20350 | 1 | Office of Naval Research 800 N. Quincy Street Arlington, Virginia 22217 Attn: Dr. Richard S. Miller | 1 |
| Commander, Naval Air Systems Command Department of the Navy Washington, D.C. 20360 Attn: Code 310C (H. Rosenwasser) | 1 | Naval Ship Research and Development Center Annapolis, Maryland 21401 Attn: Dr. G. Bosmajian Applied Chemistry Division | 1 |
| | | Naval Ocean Systems Center San Diego, California 92132 Attn: Dr. S. Yamamoto, Marine Sciences Division | 1 |

TECHNICAL REPORT DISTRIBUTION LIST, 051B

| | <u>No.</u> <u>Copies</u> | | <u>No.</u> <u>Copies</u> |
|--|-----------------------------|--|-----------------------------|
| Professor K. Wilson University of California, San Diego Department of Chemistry, B-014 La Jolla, California 92093 | 1 | Dr. B. Vonnegut State University of New York Earth Sciences Building 1400 Washington Avenue Albany, New York 12203 | 1 |
| Professor C. A. Angell Purdue University Department of Chemistry West Lafayette, Indiana 47907 | 1 | Dr. Hank Loos Laguna Research Laboratory 21421 Stans Lane Laguna Beach, California 92651 | 1 |
| Professor P. Meijer Catholic University of America Department of Physics Washington, D.C. 20064 | 1 | Dr. John Latham University of Manchester Institute of Science & Technology P.O. Box 88 Manchester, England M601QD | 1 |
| Dr. S. Greer Chemistry Department University of Maryland College Park, Maryland 20742 | 1 | | |
| Professor P. Delahay New York University 100 Washington Square East New York, New York 10003 | 1 | | |
| Dr. T. Ashworth South Dakota School of Mines & Technology Department of Physics Rapid City, South Dakota 57701 | 1 | | |
| Dr. G. Gross New Mexico Institute of Mining & Technology Socorro, New Mexico 87801 | 1 | | |
| Dr. J. Kassner University of Missouri - Rolla Space Science Research Center Rolla, Missouri 65401 | 1 | | |
| Dr. J. Telford University of Nevada System Desert Research Institute Lab of Atmospheric Physics Reno, Nevada 89507 | 1 | | |